

Parametric Analysis and Modeling of Jerusalem cross Frequency Selective Surface

Payal Majumdar*, Zhiya Zhao, Chunlin Ji, Ruopeng Liu

State Key Laboratory of Meta-RF Electromagnetic Modulation Technology, Kuang-Chi Institute of Advanced Technology, Shenzhen, China

Abstract In this study, we present the analysis and modeling of Jerusalem cross frequency selective surfaces adopting vector fitting procedure that ensures high accuracy with arbitrary terminal conditions. The simulations of microstructure are performed with full wave simulation tool CST Microwave Studio on single - layer and multilayer substrates with permittivity ranges from 2.2 - 4.3 in the frequency range 1 GHz – 30 GHz and substrate thickness ranges from 0.5 mm – 2 mm for different physical parameters. Then circuit models are extracted and developed using the vector fitting tool and implemented in a circuit simulator along with effect of polarization and angle of incidence. Then ADS SPICE generator is used for verifying circuit models developed using simulated results. The developed model is within 1% of average deviation against reference data.

Keywords Equivalent Circuit Model, Frequency Selective Surface, Jerusalem Cross, Parametric Analysis, Vector Fitting technique

1. Introduction

A Frequency Selective Surface (FSS) is a periodic, planar assembly of generally metallic elements on a dielectric layer. It is built in conjunction with the EM waves in order to "tailor" an electromagnetic link in the free-space environment. Acting as a barrier for the waves propagating along the link, the FSS controls the flow of the EM energy. FSS has been an important topic because of their comprehensive applications, such as polarizers, filters, sub-reflectors, hybrid radomes, etc. [1, 2]. Nowadays hybrid -element based FSS structures are used to achieve significant bandwidth for airborne radome applications [3]. Several analytical or numerical electromagnetic methods (FEM, FDTD or MoM) have been used to analyze FSS. One of the simplest methods is the equivalent circuit model [3-12, 14]. The low computational effort required by the equivalent circuit method allows a faster design and analysis of FSS microstructures. Moreover, the approximate analysis, based on the parallel between real structure and a lumped - RLC - network counterpart is also useful for acquiring physical insights into the working principles of FSS [6].

Unlike traditional microwave filters, the frequency response of FSS are not only functions of frequency, but also

functions of incident angle and polarizations of EM waves. Consequently, it is necessary that an excellent FSS should provide stable performances for both various incidence angles and different polarizations within its operating frequencies. A new paradigm for designing modern multifunction structurally integrated array radars for low Radar Cross Section (RCS) platforms is the use of multilayer structures with integrated radomes and FSS's. Thus, there is a growing demand for developing an accurate circuit model for FSS so that one can synthesize a desired frequency response by an optimization method in a reasonably short time using a circuit simulator [6].

In this paper, an equivalent circuit model for the analysis of Jerusalem cross (JC) has been presented, as shown in Fig.1. Being stable over wide range of parameters, the choice of JC-element allows the designer to tune its EM characteristics over the desired frequency range [3]. The simulations of microstructure are performed with full wave simulation tool CST Microwave Studio [19] on single -layer and multilayer substrates with permittivity ranges from 2.2 - 4.3 in the frequency range 1 GHz – 30 GHz and substrate thickness ranges from 0.5 mm – 2 mm for different physical parameters. The multilayer configuration of JC, as shown in Fig. 1(c), which consists of two FSS layers printed on both sides of a substrate are considered for study. The vector fitting (VF) technique [15-17] is used for determination of their poles and residues from simulated S-parameters [18]. Then the SPICE - compatible equivalent circuit model [13] of frequency-domain responses approximated by rational functions are developed. The transmission and reflection

* Corresponding author:

payalmajumdar.udsc@gmail.com (Payal Majumdar)

Published online at <http://journal.sapub.org/ijea>

Copyright © 2016 Scientific & Academic Publishing. All Rights Reserved

properties of JC FSS are evaluated through a simple and accurate circuit approach. The developed model is within 1% of average deviation against reference data.

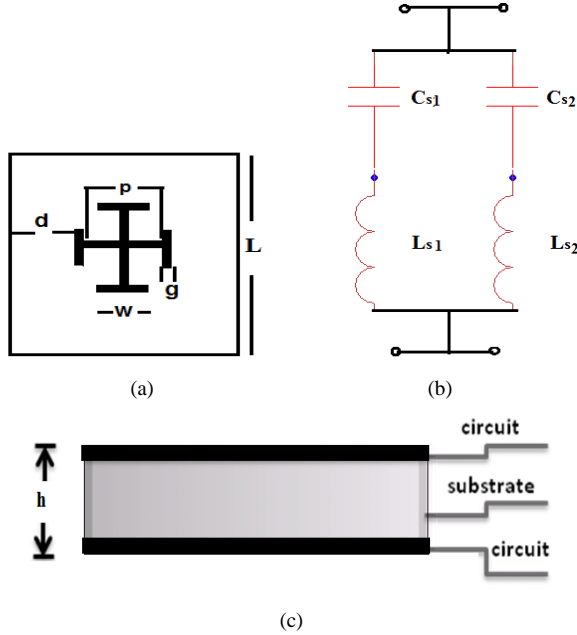


Figure 1. (a) Layout of JC (b) its equivalent circuit and (c) Multilayer configuration with side view of the FSS

2. Vector Fitting Methodology

An efficient broadband modeling of transmission lines must also take into account the frequency - dependent behaviour of dielectrics. These effects materialize as a frequency domain variation in the resistance, inductance and capacitance matrices used in the formulation of the model. In practice, the frequency dependent responses are obtained via calculation or measurements as discrete functions of frequency [17].

An attempt at formulating a general fitting methodology was introduced as VF method. Consider the rational function approximation [15]

$$f(s) = \sum_{n=1}^N \frac{c_n}{s - a_n} + d + sh \quad (1)$$

The residues c_n and poles a_n are either real quantities or come in complex conjugate pairs, while d and h are real. The problem at hand is to estimate all coefficients in equation - (1) so that a least squares approximation of $f(s)$ is obtained over a given frequency interval.

Vector fitting solves the equation-(1) sequentially as a linear problem in two stages, both times with known poles [15, 16]. The first stage was carried out with complex poles distributed over the frequency range of interest. In addition, an unknown frequency dependent scaling parameter was

introduced which permitted the scaled function to be accurately fitted with the prescribed poles. From the fitted function a new set of poles were obtained and then used in the second stage in the fitting of the unscaled function. This method ensures that the poles of the generated closed-form responses are stable or all poles have non-positive real parts.

In this section, circuit representation for complex pairs is presented for the generation of SPICE [13] compatible equivalent circuit of JC FSS from three-dimensional models. In the rational approximation of a transfer function $f(s)$, as shown in equation-(1), the n^{th} residue and pole have been extracted by using a fitting procedure mentioned in [14-16]. It has been assumed that the constant term d and the s -proportional one can be synthesized with a resistance and a capacitance whose values are $1/d$ and h . It is convenient to distinguish the case of real poles from that of complex pairs. The detailed methodology and expressions can be obtained from [13].

2.1. Real Poles

The admittance of a series RL circuit represented in Fig. 2(a) to synthesize a function $f(s)$ with a real pole is given by:

$$\bar{Y}_{RL}(s) = \frac{I(s)}{V(s)} = \frac{1}{(R + sL)} = \frac{\frac{1}{L}}{\left(s + \frac{R}{L}\right)} \quad (2)$$

Its pole and residue are

$$a_{RL} = \frac{-R}{L} \quad c_{RL} = \frac{1}{L} \quad (3)$$

Given a pair of a pole and residue extracted by a VF procedure, the corresponding couple of R and L parameters are

$$L = \frac{1}{c_{RL}} \quad R = -a_{RL}L = -\frac{a_{RL}}{c_{RL}} \quad (4)$$

2.2. Complex Pole Pair

Assume the pairs of complex and conjugate residues and poles be c_1, c_2, a_1 and a_2 respectively. The corresponding transfer function $f(s)$ is [13]:

$$f(s) = \frac{c_1}{(s - a_1)} + \frac{c_2}{(s - a_2)} = \frac{ms}{s^2 + sq + r} + \frac{p}{s^2 + sq + r} \quad (5)$$

where

$$\begin{aligned} m &= c_1 + c_2; & p &= -(c_1 a_2 + c_2 a_1) \\ q &= -(a_1 + a_2); & r &= a_1 a_2 \end{aligned} \quad (6)$$

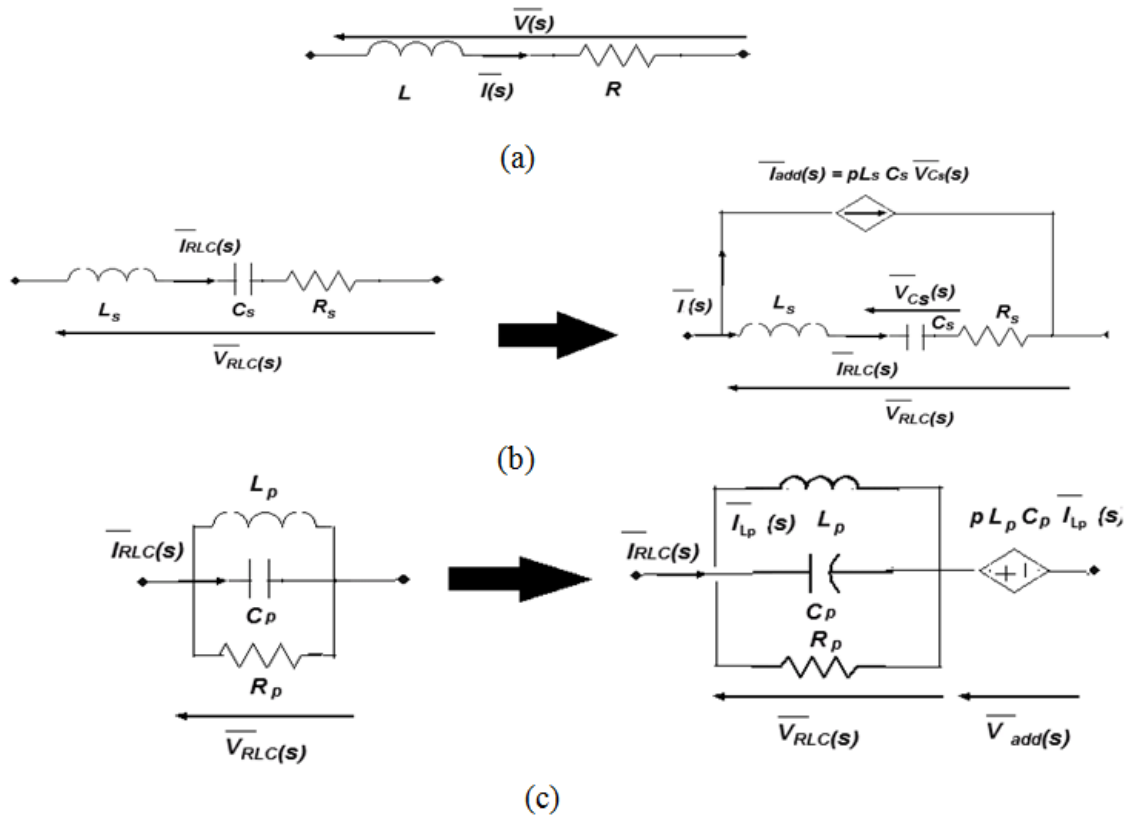


Figure 2. (a) Equivalent RL circuit for real pole synthesis; (b) Equivalent series RLC circuit; and (c) Equivalent parallel RLC circuit for complex pole pair synthesis [14]

2.2.1. Series RLC Circuit

The improved transfer function $f(s)$ of a series RLC circuit, to develop its equivalent circuit for complex pole pair synthesis [13], as shown in Fig.2(b), is written in terms of its residues and poles as

$$f(s) = \frac{ms}{s^2 + sq + r} + \frac{p}{s^2 + sq + r} \tag{7}$$

$$= Y_{RLC}(s) + f_{add}(s)$$

where,

$$\bar{Y}_{RLC}(s) = \frac{\bar{I}_{RLC}(s)}{\bar{V}_{RLC}(s)} = \frac{1}{(R + sL + \frac{1}{sC})} \tag{8}$$

$$= \frac{ms}{s^2 + sq + r}$$

in which

$$m_{1,2} = \frac{-R_s}{2L_s} \pm j \sqrt{\frac{1}{L_s C_s} - \left(\frac{R_s}{2L_s}\right)^2} \text{ with } \left(\frac{R_s}{2L_s}\right)^2 < \frac{1}{L_s C_s}$$

$$c_1 = \frac{a_1}{L_s}; \quad c_2 = \frac{a_2}{L_s} \tag{9}$$

Therefore, R_s , L_s , C_s and $f_{add}(s)$ parameters from the equivalent circuit can be evaluated as

$$R_s = -\left(\frac{a_1 + a_2}{c_1 + c_2}\right) \quad L_s = \frac{1}{(c_1 + c_2)}$$

$$C_s = \left(\frac{c_1 + c_2}{a_1 a_2}\right) \tag{10}$$

$$f_{add}(s) = p \left(\frac{1}{s^2 + s \frac{R_s}{L_s} + \frac{1}{L_s C_s}} \right)$$

2.2.2. Parallel RLC Circuit

The improved transfer function $f(s)$ of a parallel RLC circuit, to develop its equivalent circuit for complex pole pair

synthesis [13], as shown in Fig.2(c), is written in terms of its residues and poles as

$$f(s) = \frac{ms}{s^2 + sq + r} + \frac{p}{s^2 + sq + r} \quad (11)$$

$$= Z_{RLC}(s) + f_{add}(s)$$

$$\bar{Z}_{RLC}(s) = \frac{\bar{V}_{RLC}(s)}{\bar{I}_{RLC}(s)} = \frac{\frac{s}{C_p}}{\left(s^2 + s\frac{1}{R_p C_p} + \frac{1}{L_p C_p}\right)} \quad (12)$$

$$= \frac{ms}{s^2 + sq + r}$$

in which

$$m_{1,2} = -\frac{1_s}{2R_p C_p} \pm j\sqrt{\frac{1}{L_p C_p} - \left(\frac{1}{2R_p C_p}\right)^2} \quad (13)$$

$$\text{with } \left(\frac{1}{2R_p C_p}\right)^2 < \frac{1}{L_p C_p}$$

$$c_1 = \frac{\frac{a_1}{C_p}}{a_1 - a_2}; \quad c_2 = \frac{\frac{a_2}{C_p}}{a_2 - a_1}$$

in which the values of the lumped elements of the parallel RLC circuit in Fig.2(c) are

$$R_p = -\left(\frac{c_1 + c_2}{a_1 + a_2}\right) \quad C_p = \frac{1}{(c_1 + c_2)}$$

$$L_p = \left(\frac{c_1 + c_2}{a_1 a_2}\right) \quad (14)$$

$$f_{add}(s) = p \left(\frac{1}{s^2 + s\frac{1}{R_p C_p} + \frac{1}{L_p C_p}} \right)$$

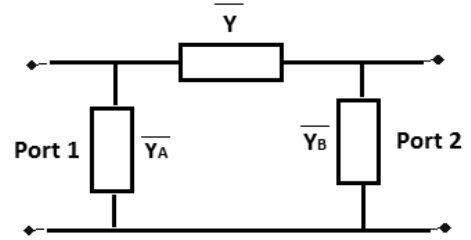


Figure 3. Equivalent Pi circuit

The following synthesis approach has been used in this research work to achieve the SPICE-compatible equivalent circuit of JC FSS microstructure [18]:

- Step 1) Scattering parameter extraction by means of a full - wave electromagnetic simulation of FSS microstructure. In this work CST Microwave Studio is used;
- Step 2) ABCD parameters evaluation;
- Step 3) Building of the Pi equivalent circuit as shown in Fig.3;
- Step 4) Residues and poles extraction of admittances \bar{Y}_A , \bar{Y}_B and \bar{Y} ;
- Step 5) SPICE-compatible equivalent circuit synthesis [13].

The VF technique has been adopted to extract poles and residues of admittances \bar{Y}_A , \bar{Y}_B and \bar{Y} , which have been synthesized in the equivalent circuit, as shown in Fig. 4, of FSS microstructure and simulated in a ADS SPICE [20] environment enabling both time and frequency analyses according to this approach [21-22].

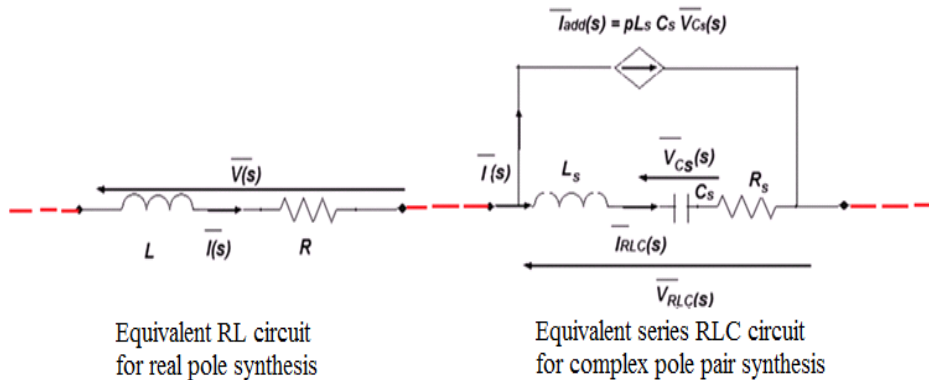


Figure 4. Proposed equivalent circuit for JC FSS using VF

3. Parametric Study of JC FSS

The full-wave approach is necessary to establish the relationship between the physical parameters of the miniaturized unit cell and the lumped elements of the circuit

model. So, JC FSS structure is studied and investigated on single-layer and multilayer substrates for different physical parameters using CST Microwave Studio [19].

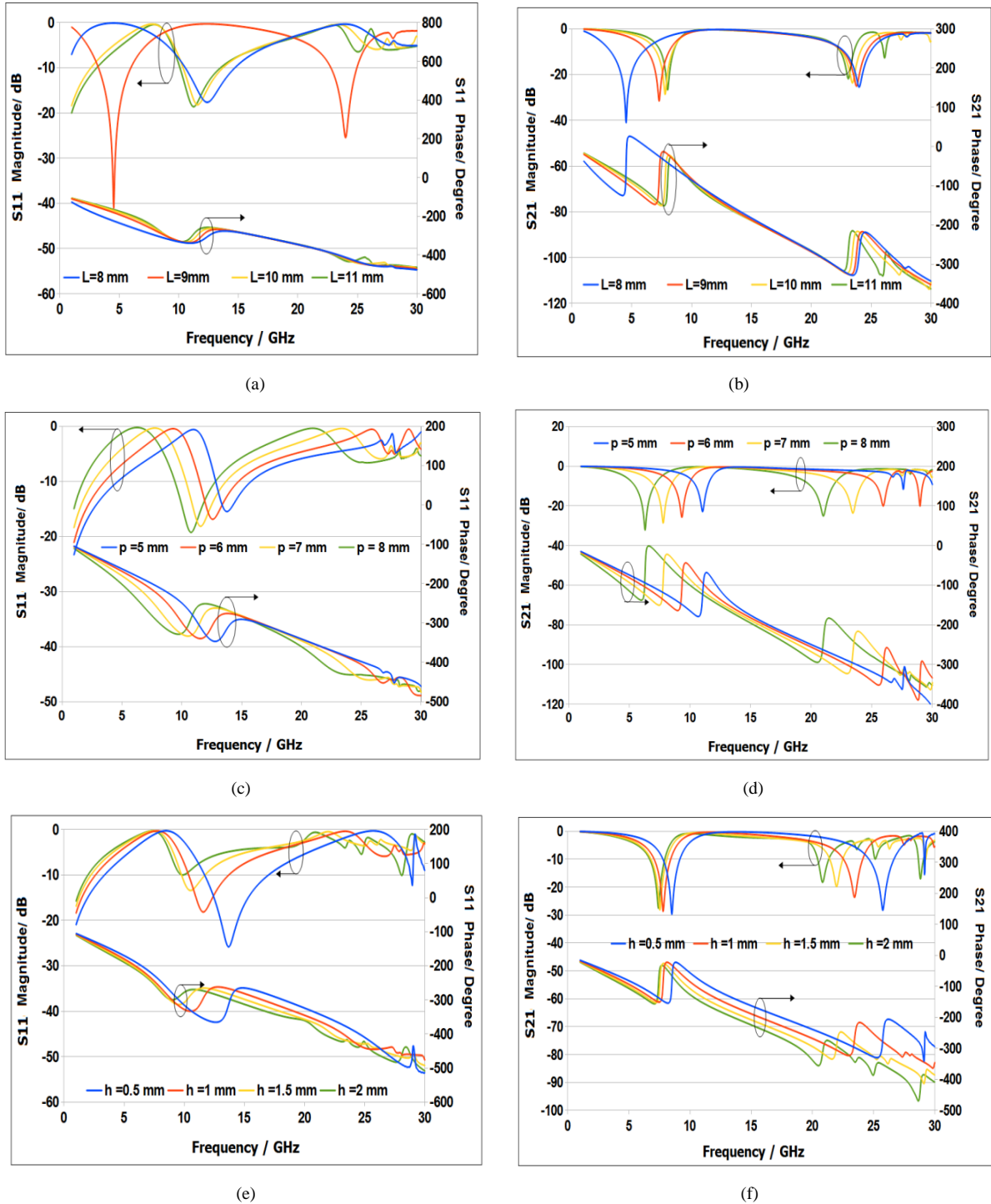


Figure 5. Plane-wave reflection and transmission response at normal incidence for JC FSS

The effects of oblique incidence and *TE* / *TM* polarization are also studied. *TM* - incidence occurs when the *E*-field is polarized parallel to the plane of incidence, i.e. $\theta = 0^\circ$, and *TE* - incidence when the *E*-field is perpendicular to the plane of incidence, i.e. $\Phi = 0^\circ$. The geometrical parameters of the designed JC FSS are: $w = 3.5$ mm, $g = 0.5$ mm, $d = 1$ mm, $p = 7$ mm and $L = 10$ mm on *FR4* substrate with permittivity $\epsilon_r = 4.4$, loss tangent $\tan \delta = 0.025$ and substrate thickness $h = 1$ mm.

Fig. 5 shows the parametric study of JC FSS at normal, in terms of varying cell size, cross size and substrate thickness. Fig.5(a) and 5(b) show magnitude and phase of reflection and transmission characteristics respectively for different cell sizes. It can be observed that by decreasing cell size there is shift in resonance peak towards lower frequency for transmission characteristics.

Fig.5(c) and 5(d) show magnitude and phase of reflection and transmission characteristics respectively for different cross sizes. By increasing cross size there is shift in resonance towards lower frequency.

It can be observed that by increasing cross size there is shift in resonance towards lower frequency. Similarly,

Fig.5(e) and 5(f) show magnitude and phase of reflection and transmission characteristics respectively for different substrate thicknesses. By increasing substrate thickness, there is shift in resonance towards lower frequency.

Fig. 6 shows the effect of oblique incidence and *TE*/*TM* polarization on magnitude and phase of reflection and transmission characteristics of JC FSS. The effect of substrate is also investigated through comparing the frequency responses of three different substrates namely - 1) *FR4* with $\epsilon_r = 4.4$ and $\tan \delta = 0.025$; 2) Roger RT5880 with $\epsilon_r = 2.2$ and $\tan \delta = 0.008$ and 3) Epoxy with $\epsilon_r = 3.6$ and $\tan \delta = 0.012$, in the frequency range 1 GHz – 30 GHz and substrate thickness ranges from 0.5 mm – 2 mm, as shown in Fig.7. The results indicate that one can take advantage of low permittivity substrates to change or improve the frequency response of the designed filter. Fig.7(a) shows the effect of different substrates on reflection characteristics of multilayer JC FSS. Fig.7(b) and 7(c) show the effect of oblique incidence and *TE*/*TM* polarization on magnitude of reflection characteristics of multilayer JC FSS.

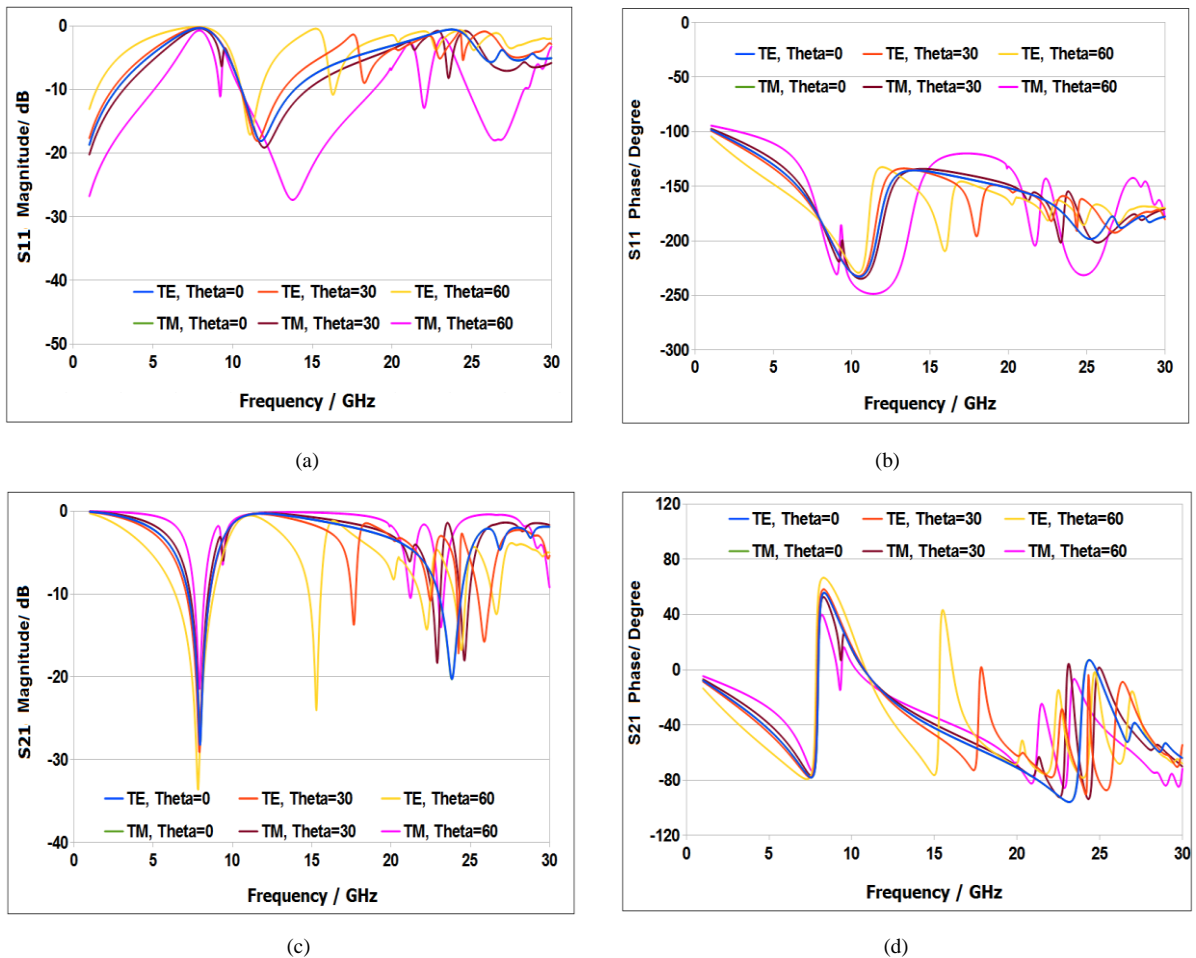


Figure 6. Plane-wave reflection and transmission response at oblique incidence for JC FSS

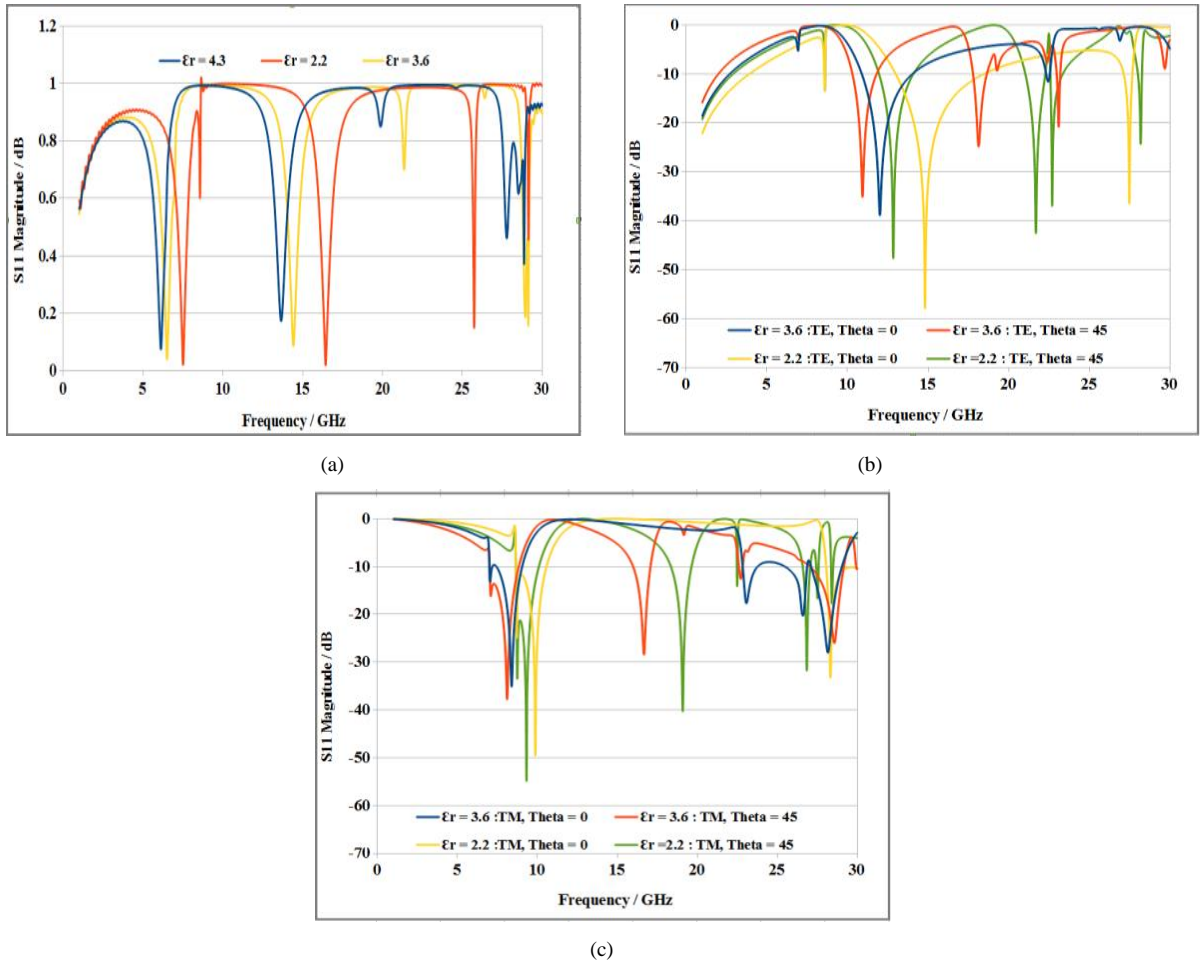


Figure 7. Plane-wave reflection and transmission response for multilayer JC FSS

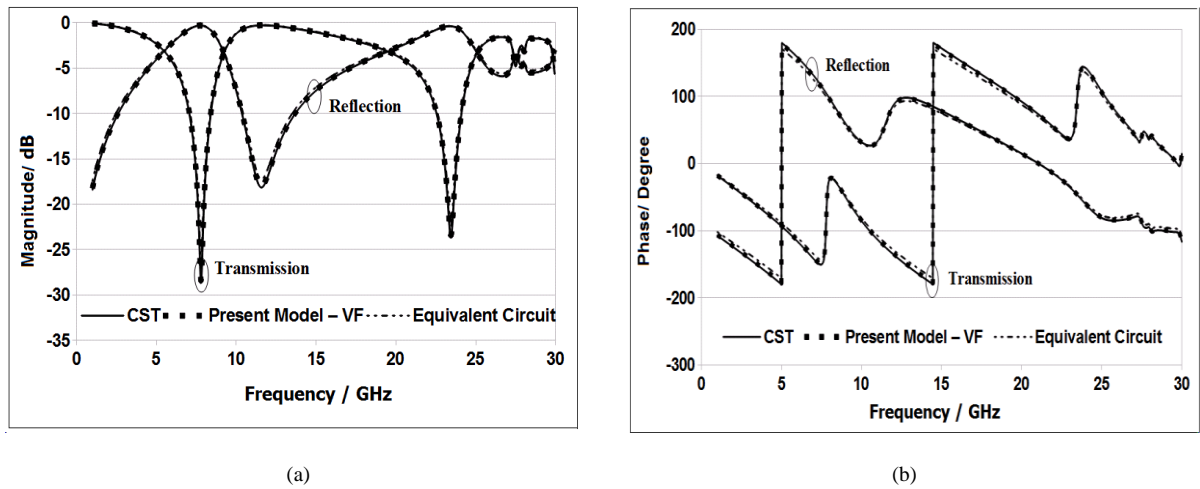


Figure 8. JC FSS - (a) Magnitude and (b) Phase

Table 1. Extracted Poles and Synthesized component values of JC FSS

Poles	Poles	R_s [Ω]	L_s [H]	C_s [F]	$\rho L_s C_s$ [S]
-0.0166e+11	r_1	5.00e-003	1.10e-011		
-1.1793e+11	r_2	2.89e+004	1.74e-006		
(-0.1147+0.0693i)e+11	c_1	2.51e-003	5.50e-012	1.28e-008	2.84e-002
(-0.1147-0.0693i)e+11	c_2	2.51e-003	5.50e-012	3.19e-009	7.09e-003
(-0.1057+0.1763i)e+11	c_3	2.51e-003	5.50e-012	1.42e-009	3.15e-003
(-0.1057-0.1763i)e+11	c_4	2.51e-003	5.50e-012	7.98e-010	1.77e-003
(-0.0078+0.2188i)e+11	c_5	2.51e-003	5.50e-012	5.11e-010	1.13e-003
(-0.0078-0.2188i)e+11	c_6	2.51e-003	5.50e-012	3.55e-010	7.88e-004
(-0.0920+1.0949i)e+11	c_7	2.51e-003	5.50e-012	2.61e-010	5.79e-004
(-0.0920-1.0949i)e+11	c_8	2.51e-003	5.50e-012	1.99e-010	4.43e-004
(-0.1287-1.163i)e+11	c_9	2.51e-003	5.50e-012	1.58e-010	3.50e-004
(-0.1287+1.163i)e+11	c_{10}	2.51e-003	5.50e-012	1.28e-010	2.82e-004

4. Model Verification and Results

In this section, the results of reflection and transmission characteristics of JC FSS obtained from the developed circuit model using VF tool, circuit model available from literature and CST simulations are compared against each other.

The reflection and transmission characteristics of JC FSS have been fitted by using 12 poles [14, 17]. The fitting procedure has provided two real poles and five complex pairs, which can be synthesized in ADS SPICE generator using repeated units shown in Fig.4. Table 1 shows extracted poles and synthesized component values of JC FSS. Fig. 8 shows the plots of the magnitude and phase of reflection and transmission characteristics, those obtained by simulation, equivalent circuit from Fig.1(b) and equivalent circuit using VF technique.

The proposed synthesis allows a satisfactory approximation of all the considered FSS being the percentage errors on magnitude and phase of the order of 1%. While the equivalent circuits available in literature have the percentage errors on magnitude and phase of the order of 2%. All the equivalent circuits are designed and simulated using ADS SPICE generator.

5. Conclusions

The present work reports detailed investigation and study of JC FSS with resonant unit cells. The simulations are performed with CST Microwave Studio on single-layer and multilayer substrates for different physical parameters with permittivity ranges from 2.2 - 4.3 in the frequency range 1 GHz – 30 GHz and substrate thickness ranges from 0.5 mm – 2 mm. The VF tool is employed to extract equivalent circuits from S-parameters of JC FSS microstructure to use in circuit simulators to avoid time consuming 3D simulations. Then ADS SPICE generator is used for verifying circuit models

developed using simulated results. All the models are within 1% of average deviation against reference data. The programming has been done in MATLAB. The method is useful for developing low-profile antenna applications based on FSS microstructures.

ACKNOWLEDGEMENTS

This research work has been supported by grants from State Key Laboratory of Meta-RF Electromagnetic Modulation Technology (No. 2011DQ782011), Guangdong Province Engineering Laboratory for Millimeter Wave Meta-RF (No.1111), Shenzhen Key Laboratory of Data Science and Modeling (No. CXB201109210103A), Shenzhen Science and Technology Plan (No. JC201105201150A) and Shenzhen Science and Technology Plan (No. ZD201111080127A).

REFERENCES

- [1] B.A. Munk, Frequency-selective surfaces: Theory and Design, Wiley, New York, 2000.
- [2] S.S. Suganya and T.R. Suresh Kumar, "Design of Frequency Selective Surfaces Filter-A Review" International Journal of Innovative Research in Science, Engineering and Technology, Vol. 4, Special Issue 6, pp.916-920, May 2015.
- [3] Sruthi T.V., Sangeetha B., K. S. Divya, Shiv Narayan, "A Novel Hybrid-Element FSS For Radome Applications", International Journal of Industrial Electronics and Electrical Engineering, ISSN: 2347-6982, Vol.4, Issue-3, pp.50-53, Mar. 2016.
- [4] I. J. Bahl, "Lumped elements for RF and microwave circuits," Artech House Inc. 2003.

- [5] R.J. Langley and E.A. Parker, "Equivalent-Circuit Models for Frequency-Selective Surfaces at Oblique Angle of Incidence," *IEE Proc.*, Vol. 18, No. 7, pp.294-296, Apr. 1982.
- [6] F. Costa, A. Monorchio and G. Manara, "Efficient Analysis of Frequency-Selective Surfaces by a Simple Equivalent-Circuit Model," *IEEE Antenna and Propagation Magazine*, Vol. 54, pp. 35-48, 2012.
- [7] C.K. Lee and R.J. Langley, "Equivalent- Circuit Models for Frequency-Selective Surfaces at oblique angle of incidence," *IEE Proc*, Vol. 132, pp.395-399, 1985.
- [8] R.J. Langley and A.J. Drinkwater, "An Improved Empirical Model for the Jerusalem Cross," *IEE Proc.*, Part H: *Microwaves, Opt. Antenna*, Vol. 129, pp.1-6, 1982.
- [9] Y.-C. Chung, K.-W. Lee, I.-P. Hong, M.-G. Lee, H.-J. Chun and J.-G. Yook, "Simple Prediction of FSS Radome Transmission Characteristics using an FSS Equivalent Circuit Model", *IEICE Electronics Express*, Vol. 8, No. 2, pp.89-95, Jan. 2011.
- [10] K.-W. Lee, Y.-R. Jeong, I.-P. Hong, M.-G. Lee, H.-J. Chun and J.-G. Yook, "Simple Design Method of FSS Radome Analysis using Equivalent Circuit Model", *IEICE Electronics Express*, Vol. 8, No. 23, pp.2002-2009, Dec. 2011.
- [11] D. Singh, A. Kumar, S. Meena and V. Aggarwal, "Analysis of Frequency Selective Surfaces for Radar Absorbing Materials", *PIER B*, Vol. 38, pp.297-314, Feb. 2012.
- [12] Ze Yu and GuiZhen Lu, "Equivalent Circuit Method for Analyzing High Impedance Surface Based Microwave Absorbing Structure", *APS/URSI 2014 Conference*, Memphis, Tennessee, U.S.A., 2014.
- [13] G. Antonini, "SPICE Equivalent Circuits of Frequency - Domain Responses," *IEEE Trans. on Electromagnetic Compatibility*, Vol. 45, pp.502-512, 2003.
- [14] Payal Majumdar, Zhiya Zhao, Yutao Yue, Chunlin Ji and Ruopeng Liu, "Equivalent Circuit Model of Cross and Circular Ring FSS Using Vector Fitting," *3rd Asia-Pacific Conference on Antennas and Propagation, APCAP 2014*, Harbin, P.R. China, July 2014.
- [15] B. Gustavsen and A. Semlyen, "Rational approximation of frequency domain responses by Vector Fitting," *IEEE Trans. Power Delivery*, Vol. 14, pp. 1052-1061, 1999.
- [16] B. Gustavsen and A. Semlyen, "Fast passivity assessment for S-parameter rational models via a half-size test matrix," *IEEE Trans. Microwave Theory And Techniques*, Vol.56, pp. 2701-2708, 2008.
- [17] B. Gustavsen and H.M.J. De Silva, "Inclusion of Rational Models in and Electromagnetic Transient Program-Y-Parameters, Z-Parameters, S-Parameters, Transfer Functions," *IEEE Trans. Power Delivery*, Vol. 28, pp.1164-1174, 2013.
- [18] Payal Majumdar, Zhiya Zhao and Ruopeng Liu, "Equivalent Circuit Model of Jerusalem Cross FSS Using Vector Fitting," *5th International Conference on Metamaterials, Photonic Crystals and Plasmonics, META 2014*, Singapore, 2014.
- [19] CST Studio Suite v 2009, CST GmbH-Computer Simulation Technology, www.cst.com.
- [20] Agilent Advanced Design System v 2011.
- [21] Payal Majumdar, Zhiya Zhao and Ruopeng Liu, "Parametric Analysis of Different Configurations of Loop Elements in Frequency-Selective Surfaces," *Advance in Electronic and Electric Engineering*, ISSN 2231-1297, Vol.4, No.2, pp.162-167, January 2014.
- [22] Payal Majumdar, Zhiya Zhao, Chunlin Ji and Ruopeng Liu, "Equivalent Circuit Model of Multilayer Double Square Loop FSS Using Vector-Fitting," *APS/URSI 2015 Conference*, Vancouver B.C., Canada, 2015.